DESIGN AND VERIFICATION OF ULTRA-HIGH TEMPERATURE LITHIUM HEAT PIPE BASED EXPERIMENTAL FACILITY

by

Chongju HU[a,b,c], Dali YU[a*], Meisheng HE[a], Taosheng LI[a], and Jie YU[a]

[a] Institute of Nuclear Energy Safety Technology, Hefei Institutes of Physical Science, Chinese Academy of Sciences, Hefei, Anhui, China
[b] University of Science and Technology of China, Hefei, Anhui, China
[c] Suzhou University, Suzhou, Anhui, China

Original scientific paper
https://doi.org/10.2298/TSCI210528263H

Lithium heat pipe has broad applications in heat pipe cooled reactors and hypersonic vehicles due to its ultra-high working temperature which is around 1700 K. In this paper, a lithium heat pipe based experimental facility has been designed to test the heat transfer performance of the lithium heat pipe. A simplified mathematical model of heat pipe has been implemented into a CFD approach, which is used to verify the design of lithium heat pipe and its experimental facility. Results showed that the CFD approach is in good agreements with some well-known existing models and experimental data, and deviation between the results is within 5% range. The adjustment range of mixed gas thermal resistance and cooling water flow rate was obtained by analyzing the effects of different cooling conditions on the performance of the experimental facility. It is necessary to ensure the cooling water flow rate is above 0.11 Lph to prevent water boiling when the heating power is 10 kW around, and the optimal proportion of helium is 70-90%. The operation characteristics of the lithium heat pipe under unsteady-state with varying heating power were simulated numerically. The results show that the proportion of helium must be less than 60% for normal operation of the lithium heat pipe. This work provides a reference and numerical verification for the design of lithium heat pipe based experimental facility, which can be used to reveal the heat transfer mechanisms of the lithium heat pipe during the experiment.

Key words: *lithium heat pipe, CFD, heat transfer limit, heat transfer performance,*

Introduction

As one of the most efficient heat transport devices, heat pipe has the advantage of transporting large quantities of heat through a small cross-sectional area over a considerable distance with no additional power input, and is widely applied in space, underwater, and ground nuclear reactor concepts [1-4]. University of New Mexico has developed a conceptual design of a heat pipe-segmented thermoelectric module converters space reactor power system for a net power of 110 kWe [5]. Los Alamos National Laboratory has designed a MW electric mobile heat pipe reactor for power supply in strategic defenses locations, theaters of battle, and remote communities [6]. The NASA has started a Kilopower project to develop a fission heat pipe reactor, which could be scaled from 1-10 kW for both science and human explorations

* Corresponding author, e-mail: dlyu@inest.cas.cn

[7, 8]. Westinghouse has completed the design of a megawatt heat pipe reactor evinci for off-grid Markets [9, 10].

Heat pipe is the major heat transfer element in the heat pipe cooled nuclear reactor, its heat transport characteristics determine the reactor operation performance and safety during the processes of start-up, steady-states, transients, and shut down. In the aspect of liquid filling rate, Sukchana and Jaiboonma [11] studied the impacts of filling rate on thermal efficiency of a R-134a heat pipe, and found that the optimum filling ratio is 15% when adiabatic length of the heat pipe is short. At low heating power, Mahdavi *et al.* [12] discovered that low filling volume reduces the maximum heat transfer rate of heat pipe, though the heat pipe has a low thermal resistance. What's more, high liquid filling volume increases thermal resistance of the heat pipe. Khalili and Shafii [13] explored the heat transfer performance of water heat pipes for two different kinds of sintered wick with different liquid filling rates, and found that the most suitable filling rate for both heat pipes are around 20%. Xiong *et al.* [14] indicated that molten salt heat pipe with 40 g filling amount has the fastest response in the start-up process. Lu *et al.* [15] showed that heat pipe with high filling volume can enhance the startup performance. Liu *et al.* [16] pointed out that 40% filling rate best applies when heating power is 4 kW, and 30% filling rate is most suitable when heating power is 8 W for deionized water heat pipe.

As for researches on the inclination angle, Liu *et al.* [17] discovered that CuO nanofluid heat pipe with inclination angle of 45° has maximum heat transfer performance. Kumaresan *et al.* [18] found the thermal resistance first increases and then decreases with increasing inclination angle when the evaporation is higher than the condensation for CuO nanofluid heat pipe, and the best inclination angle is also found to be 45°. Supowit *et al.* [19] found the inclination angle has significant impacts on the distribution of liquid metal film in water heat pipe. Xiong *et al.* [14] studied the heat transfer and start-up performance of molten salt heat pipe when the evaporation section is higher than the condensation section and the inclination angles are 30°, 50°, 70°, and 90°, respectively. For the heat transfer limit, Kemme [20] found that the heat pipe temperature and working fluid have great influences on the sonic limit, which is revealed through experiments on heat pipes of sodium, potassium, and cesium working fluids, respectively. Li *et al.* [21, 22] investigated the parameters affecting the evaporation/boiling and critical heat flux (CHF) from thin capillary wicking structures. Seo and Lee [23] studied the thermal hydraulic characteristics of a long deionized water heat pipe. It is found that the entrainment limit points are affected by the L/D value of the heat pipe. Wang *et al.* [24] investigated potassium heat pipe heated with constant heat flux. It was found that capillary limit and viscous limit are critical for the start-up performance. Miao *et al.* [25] studied the cooling temperature and the size effect on the CHF of water heat pipe, which indicates CHF increases with increasing cooling temperature and increasing length of the heat pipe. Baraya *et al.* [26] studied the transient thermal response of a heat pipe subjected to heat input pulses of varying duration that exceed the capillary limit. It is demonstrated that under such transient heating conditions, a heat pipe can sustain heat loads higher than the steady-state capillary limit for brief periods of time without experiencing dryout. Wang *et al.* [27] experimentally analyzed the heat transfer limit for high L/D potassium heat pipe operating with inclination angle.

Current researches mainly focused on the normal temperature and high temperature heat pipe. It is necessary to design and evaluate the heat pipe working at ultra-high temperature for better transferring heat from the nuclear reactor core. A lithium heat pipe based experimental facility has been designed and numerical approach has been used to verify the design feasibility. The operating characteristics of the lithium heat pipe and its experimental facility under different system conditions were discussed.

Design of lithium heat pipe

The design requirements of the lithium heat pipe are:
- working temperature is around 1700 K,
- heat transfer capacity is 10 kW,
- evaporation section is 320 mm,
- insulation section is 200 mm, and
- the condensation section is 320 mm.

Materials selection

Heat pipe materials should meet the requirements of compatibility with the working fluid and the requirements of strength and stiffness at the working temperature. Besides, the welding performance, environmental corrosion resistance, and economy are all important factors to be considered. Material of niobium 1% zirconium is selected as the lithium heat pipe material in this design [28, 29].

Preliminary selection of wick structure

Due to large amount of heat transfer, the selection of wick is a complex problem especially for ultra-high temperature heat pipe. In order to improve the heat transfer ability of the heat pipe, the wick is required to have a very small effective capillary radius to increase the capillary forces. Meanwhile, it also requires a large permeability to reduce the pressure drop of liquid backflow. Besides, a small thermal resistance for reducing the radial thermal resistance of the heat pipe is also one of the important factors to be considered in the selection of the wick. It is difficult to meet all the aforementioned requirements by one kind of wick. The composite wick, trunk wick, and annulus wick are good choices. The annulus wick was selected in this design [30, 31]. The preliminary selection of the structure of wick was comprised of seven layers of a 400 mesh woven screen of 25 μm diameter wires and 5 mm annulus [30]. The lithium heat pipe's structure is shown in fig. 1.

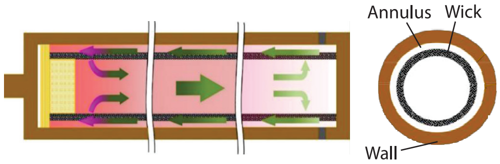

Figure 1. Schematic of the lithium heat pipe structure

Calculation of vapor chamber diameter

As for designing the vapor chamber of the lithium heat pipe, first should consider the influence of diameter on the vapor flow rate. Excessive vapor velocity will cause the compressibility effect of steam, resulting in a large axial temperature gradient. To avoid this situation, the Mach number of the vapor should not exceed 0.2 [32]. Figure 2 shows the variation of vapor Mach number with different vapor cavity diameter when the lithium heat pipe works at 1700 K.

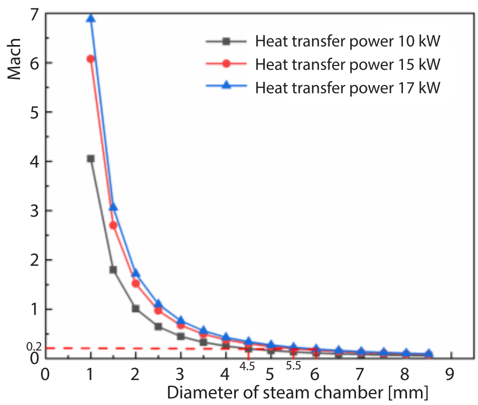

Figure 2. Mach numbers *vs.* diameter of vapor chamber

When the heat transfer power is given, the Mach number decreases with increasing diameter of the vapor chamber. The smaller the vapor chamber is, the influence of the vapor chamber

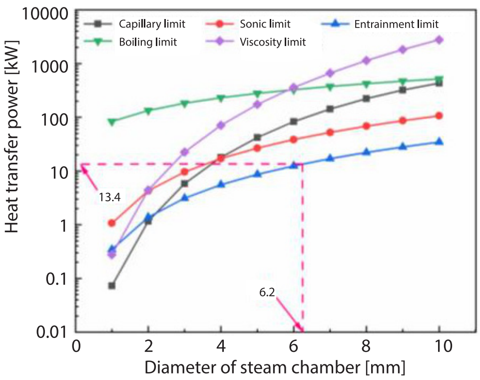

Figure 3. Effect of steam chamber diameter on heat transfer limits

diameter on the Mach number is more obvious. For the same diameter of the vapor chamber, the vapor Mach number increases with increasing heat transfer power. Under the heat transfer powers of 10 kW, 15 kW, and 17 kW, the diameter of the vapor chamber should be greater than 4.5 mm, 5.5 mm, and 6 mm, respectively. This ensures the Mach number can meet the requirement. The heat transfer performances of a heat pipe are limited by various heat transfer limits. Heat transfer limits that ultra-high temperature lithium heat pipe may encounter during working include viscosity limit, sonic limit, entrainment limit, capillary limit, and boiling limit. The lowest limit among these constraints defines the maximum heat transport limitation of a heat pipe at a given temperature. To ensure that the heat pipe can reach the required power at the design temperature, it is necessary to ensure that the heat transfer limit power of the heat pipe is higher than the required power at the design temperature. Figure 3 shows the variations of heat transfer limit of lithium heat pipe vs. different vapor chamber diameters when the lithium heat pipe works at 1700 K. This design was based on the currently accepted heat pipe design relations as compiled in [32, 33]. The capillary limit is the lowest limit of the lithium heat pipe if the diameter of the vapor chamber is less than 2 mm as shown in fig. 3. When the diameter of the vapor chamber is greater than 2 mm, the carrying limit is the lowest limit of the lithium heat pipe. To ensure safety, heat pipe design should have at least a 1/3 margin. The diameter of the vapor chamber should be greater than 6.2 mm in this design.

Optimization of the annulus of wick

The size of the annulus has an important influence on the liquid backflow in heat pipe. With the increasing annulus size, the permeability of the wick increases, which is conducive to the backflow of the fluid. However, the increase of the annulus size will lead to the increase of the radial thermal resistance, which will affect the heat transfer performance of the heat pipe. Therefore, it is necessary to optimize the size of the annulus. Figure 4 shows variations of heat transfer limits of lithium heat pipe *vs.* different annulus sizes when the heat pipe works at 1700 K. The size of the annulus does not affect viscosity limit, sonic limit, and the entrainment limit, but the boiling limit decreases with increasing annulus size. This is because the increasing annulus size will lead to the increase of the radial temperature difference of the wick, which is conducive to formation of bubbles. The capillary limit increases with increasing annulus size, and this is because the pressure drop of liquid backflow decreases with increasing annulus size.

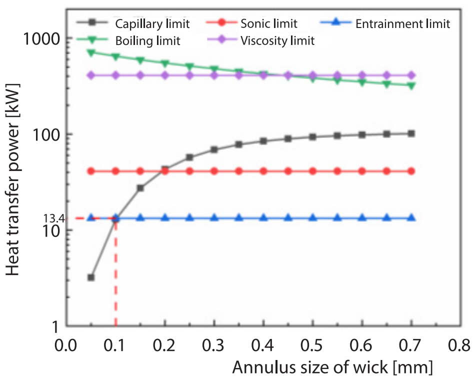

Figure 4. Heat transfer limits *vs.* different annulus sizes

When the size of the annulus is less than 0.1 mm, the heat transfer power is determined by capillary limit, and the heat transfer power increases with increasing annulus size. When the size of annulus is greater than 0.1, heat transfer power is determined by the entrainment limit, heat transfer power is not affected by the annulus size and heat transfer power is maintained at 13.4 kW. To reduce thermal resistance, the annulus size should be reduced as much as possible and annulus size is designed as 0.1 mm in this work.

Design of wall thickness

When the lithium heat pipe works at 1700 K, it needs to sustain the internal pressure, so its strength needs to be guaranteed. The shell and end-cover wall thicknesses were designed according to [32]:

$$t_1 \geq \frac{Pd_o}{2[\sigma]} \tag{1}$$

$$t_2 \geq \sqrt{\frac{Pd_o^2}{8[\sigma]}} \tag{2}$$

where t_1, t_2 [mm] are the shell wall thickness of lithium heat pipe and end-cover wall thickness of lithium heat pipe, respectively, P [Pa] – the pressure difference, d_o [mm] – the outer diameter of lithium heat pipe, and σ [Pa] – the allowable stress of heat pipe materials.

Structural parameters of the heat pipe

Based on previous analysis and considering the convenience of manufacturing, the structural parameters of the lithium heat pipe were adjusted according to the standard of niobium seamless pipe [34]. The parameters are listed in tab. 1 and fig. 5 shows the ultra-high temperature lithium heat pipe we have fabricated.

Table 1. Structural parameters of the ultra-high temperature lithium heat pipe

Parameter	Value
Material of heat pipe wall	Niobium 1% zirconium
Material of wick structure	Niobium 1% zirconium
Vapor core diameter [mm]	7.38
Thickness of wrapped screen wick [mm]	0.41
Thickness of gap [mm]	0.1
Thickness of heat pipe wall [mm]	0.3
Outer diameter of heat pipe [mm]	9
Porosity of the wick structure	0.7
Length of the heat pipe [mm]	1000
Length of the evaporator [mm]	320
Length of the condenser [mm]	480

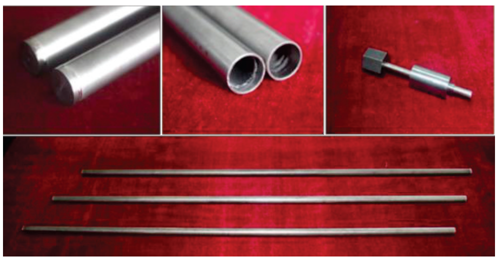

Figure 5. Experimental samples of the designed lithium heat pipe

Design of lithium heat pipe experimental facility

Figure 6 shows the schematic diagram of the lithium heat pipe experimental facility. The whole test system consists of four subsystems: heating system, cooling system, data acquisition system, and angle control system. In the heating system, heating coils are wound around the evaporation section of the lithium heat pipe, and the heating power is controlled by the heating controller. The outer layer of the whole heat pipe is covered with a quartz tube and is equipped with a vacuum pump and pressure gauge. To prevent the lithium heat pipe from oxidation at high temperatures, the vacuum pump is used before the test to ensure that the whole heat pipe test environment is maintained at a pressure level of less than 10^{-6} torr [31]. The cooling system adopts circulating water for cooling. The water source comes from the water tank. Thermocouples are installed at both the cooling water inlet and outlet for temperature measurements.

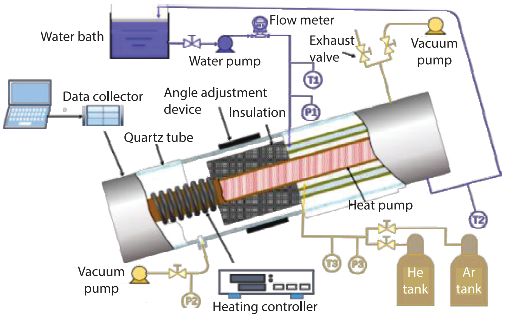

Figure 6. Schematic of lithium heat pipe experimental facility

The cooling water inlet uses a rotameter to measure the water flow and uses a pressure gauge to measure the pressure. To prevent water boiling, the hybrid helium-argon gas is used to separate the lithium heat pipe from the cooling water. Helium and argon are, respectively provided by the external gas tank. Each tank is equipped with a valve, a pressure gauge, and a temperature sensor. The hybrid helium-argon gas outlet is equipped with a vacuum pump and a vent valve. The thermal resistance of the mixed gas can be adjusted by changing the proportion of helium. The structure of the gas-water jacket is shown in fig. 7. The adiabatic section of the lithium heat pipe is wrapped by thermal insulation material. The inner layer of the insulation material adopts a rigid alumina core. The middle layer adopts silica aerogel with thermal conductivity less than 0.005 W/mK. The outer layer adopts flexible quartz fiber felt, and the flexible quartz fiber felt is wrapped with a foil reflector in the outside. The data acquisition system consists of a series of sensors, data collectors, and computers. The *B*-type thermocouple is used to measure the temperature of the outer wall of the lithium heat pipe. The thermocouple is tightly fixed in the groove of the outer wall of the lithium heat pipe to ensure measurement quality. All measurement results are collected by the data acquisition system and stored in the computer. According to the requirements of the standard [35], the distribution of temperature measurement points of the lithium heat pipe is shown in fig. 8. The angle control system is mainly composed of motor, reducer, and turnover bracket. The motor is equipped

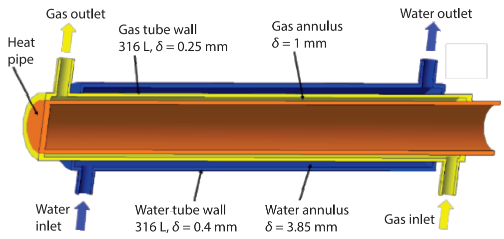

Figure 7. Structure of the gas-water jacket

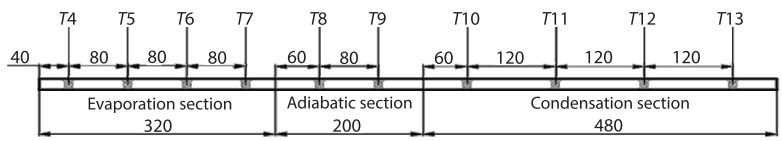

Figure 8. Distribution of temperature measurement points of lithium heat pipe

with a brake, so there is no need to provide additional support after power failure. The turnover bracket adopts a single cantilever structure for convenient operation. The angle control system can realize 0°-180° turnover.

Numerical simulation and verification

The numerical simulations mainly consist of the lithium heat pipe and gas-water jacket. The simulation of the gas-water jacket is relatively simple and easy to realize. However, the modelling of the lithium heat pipe is very complex because it involves phase transition and porous medium flow. Therefore, it is necessary to establish a simplified physical model for the lithium heat pipe, and verify the correctness of the model by experimental data.

Numerical simulation of the lithium heat pipe

Mathematical model of lithium heat pipe

According to the heat transfer characteristics of the lithium heat pipe, the lithium heat pipe is divided into wall section, wick section, and vapor section. In the wall section, the heat transfer mode is conduction. The governing equations of the wall section for steady-state and transients are given:

$$0=\frac{1}{r}\frac{\partial}{\partial r}\left(k_{\mathrm{w}}r\frac{\partial T}{\partial r}\right)+\frac{\partial}{\partial z}\left(k_{\mathrm{w}}\frac{\partial T}{\partial z}\right)+\frac{1}{r^2}\frac{\partial}{\partial \varphi}\left(k_{\mathrm{v}}\frac{\partial T}{\partial \varphi}\right) \tag{3}$$

$$C_{\mathrm{w}}\frac{\partial T}{\partial t}=\frac{1}{r}\frac{\partial}{\partial r}\left(k_{\mathrm{w}}r\frac{\partial T}{\partial r}\right)+\frac{\partial}{\partial z}\left(k_{\mathrm{w}}\frac{\partial T}{\partial z}\right)+\frac{1}{r^2}\frac{\partial}{\partial \varphi}\left(k_{\mathrm{v}}\frac{\partial T}{\partial \varphi}\right) \tag{4}$$

where C_{w} [Jm^{-3}K^{-1}] is the volumetric heat capacity of the wall material, k_{w} [Wm^{-}1K^{-1}] – the thermal conductivity of the wall material, and r, z, and φ [m] are the radial co-ordinate, axial co-ordinate, and circumferential co-ordinate, respectively. The lithium filled in the wick is solid at room temperature, and gradually melts and turns into liquid with increasing temperature. The analysis of lithium heat pipe in this paper are implemented both on the steady-state conditions and power shifting transients. The lithium working fluid is in a liquid state during the whole working process, so the melting of lithium is not considered in the analysis of the wick region. Moreover, the liquid lithium in the wick flows from the condensation section the evaporation section driven by the capillary force. As the density of the liquid lithium is much greater than that of the vapor lithium, the velocity of liquid lithium in the wick is very small. The effect of flow on heat transfer, which means convective heat transfer, can be ignored. Therefore, the wick section is regarded as a pure heat conduction model [36]. The governing equations of the wick section for steady-state and transients are:

$$0=\frac{1}{r}\frac{\partial}{\partial r}\left(kr\frac{\partial T}{\partial r}\right)+\frac{\partial}{\partial z}\left(k\frac{\partial T}{\partial z}\right)+\frac{1}{r^2}\frac{\partial}{\partial \varphi}\left(k\frac{\partial T}{\partial \varphi}\right) \tag{5}$$

$$C\frac{\partial T}{\partial t}=\frac{1}{r}\frac{\partial}{\partial r}\left(kr\frac{\partial T}{\partial r}\right)+\frac{\partial}{\partial z}\left(k\frac{\partial T}{\partial z}\right)+\frac{1}{r^2}\frac{\partial}{\partial \varphi}\left(k\frac{\partial T}{\partial \varphi}\right) \tag{6}$$

The coefficients C, and k in eqs. (5) and (6) are given, respectively:

$$C=\begin{cases} C_l & \text{annular section of wick} \\ \varepsilon C_l+(1-\varepsilon)C_{\mathrm{s}} & \text{wrapped screen section of wick} \end{cases} \tag{7}$$

$$k = \begin{cases} k_l & \text{annular section of wick} \\ \dfrac{k_l[(k_l + k_s) - (1-\varepsilon)(k_l - k_s)]}{[(k_l + k_s) + (1-\varepsilon)(k_l - k_s)]} & \text{wrapped screen section of wick} \end{cases} \tag{8}$$

where C [Jm^{-3}K^{-1}], k [W^{-1}K^{-1}] are the effective volumetric heat capacity and the effective thermal conductivity of wick, C_l [Jm^{-3}K^{-1}], k_l [Wm^{-1}K^{-1}] – the volumetric heat capacity and the thermal conductivity of the annulus section of wick, C_s [Jm^{-3}K^{-1}], k_s [Wm^{-1}K^{-1}] – the volumetric heat capacity and the thermal conductivity of the wrapped screen section of wick, ε – represents the porosity of wick, and r, z, and φ [m] represent radial co-ordinate, axial co-ordinate, and circumferential co-ordinate, respectively. During the heat pipe start up from the frozen state, the flow in the vapor region can be categorized by three-stages with increasing temperature: free molecular flow, rarefied vapor flow, and continuous flow [37]. When lithium heat pipe completes the start-up process, continuous flow has been established. Therefore, the thermal resistance of the vapor region is very small relative to other sections. It can be simplified as heat conduction with high thermal conductivity. The governing equations of the vapor section when the lithium heat pipe works at the steady-state operation under the design condition and the variable power unsteady operation are shown:

$$C_v \frac{\partial T}{\partial t} = \frac{1}{r}\frac{\partial}{\partial r}\left(k_v r \frac{\partial T}{\partial r}\right) + \frac{\partial}{\partial z}\left(k_v \frac{\partial T}{\partial z}\right) + \frac{1}{r^2}\frac{\partial}{\partial \varphi}\left(k_v \frac{\partial T}{\partial \varphi}\right) \tag{9}$$

$$0 = \frac{1}{r}\frac{\partial}{\partial r}\left(k_v r \frac{\partial T}{\partial r}\right) + \frac{\partial}{\partial z}\left(k_v \frac{\partial T}{\partial z}\right) + \frac{1}{r^2}\frac{\partial}{\partial \varphi}\left(k_v \frac{\partial T}{\partial \varphi}\right) \tag{10}$$

The coefficients k_v in eqs. (9) and (10) are given by eq. (11).

$$k_v = \text{constant} \tag{11}$$

where C_v [Jm^{-3}K^{-1}] is the volumetric heat capacity of the lithium vapor, k_v [Wm^{-1}K^{-1}] – the thermal conductivity of the lithium vapor and constant is a large constant, and r, z, and φ [m] are the radial co-ordinate, axial co-ordinate, and circumferential co-ordinate, respectively.

Numerical approach

The CFD software FLUENT is used to simulate the lithium heat pipe. A 1/2 3-D symmetrical model of lithium heat pipe is established and shown in the fig. 9. According to the analysis in section *Mathematical model of lithium heat pipe*, the corresponding physical properties for different sections of the lithium heat pipe are applied, respectively. Grid sensitivity analysis has been done to obtain the fine mesh.

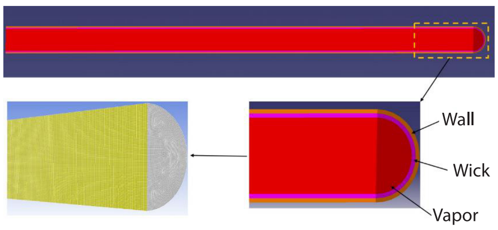

Figure 9. Mesh model of the lithium heat pipe

Verification of heat pipe model

To verify the correctness of the heat pipe model, the simulated results by CFD are compared with the results of other existing models in literatures [38-40]. Among which, Faghri and Harley [39] adopt lumped parameter method, Cao and Faghri [40] adopt transient network method, and Zuo and Faghri [38] adopt 2-D method. The comparison results are shown in fig. 10. It is obvious to see from the comparisons that the CFD results by FLUENT are in good agreement with the existing models and difference between them is in the range of ~2%.

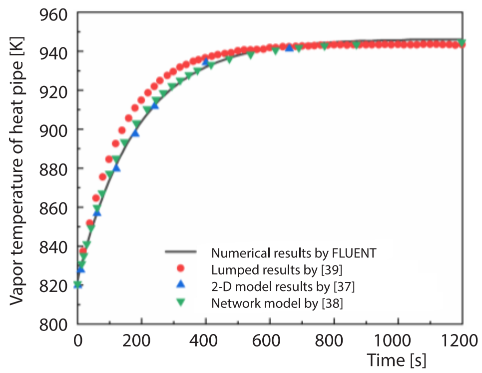

Figure 10. Comparisons between FLUENT and existing models

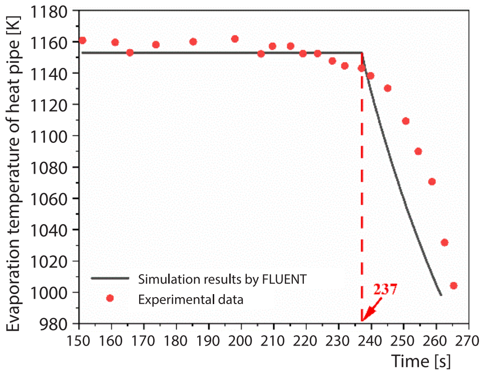

Figure 11. Validation of numerical model with experimental

The numerical model is used to calculate a lithium heat pipe we have tested in another facility. The lithium heat pipe has two layers of 200 mesh wrapped screen wick, and a 1 mm-thick wall. The heat pipe is 1 m in length and 18 mm for outer diameter. The evaporation section of the lithium heat pipe was uniformly heated with a power of 2.1 kW, and the condensation section has thermal radiation with emissivity of 0.7. When the heating time was 150 seconds, the heat pipe reaches a stable state, and after 237 seconds, the heating power was reduced to 0. Figure 11 shows the numerical results compared with the corresponding experimental data and difference between them is about ~5%.

Numerical simulation of the experimental facility

Geometries and mesh of the experimental facility

The numerical model of the lithium heat pipe experimental facility is mainly composed of the lithium heat pipe and gas-water jacket. The whole model is composed of a 1/2 3-D symmetrical model, and the simplified lithium heat pipe model in section *Numerical simulation of the lithium heat pipe*. Figure 12 shows the numerical simulation of the experimental facility.

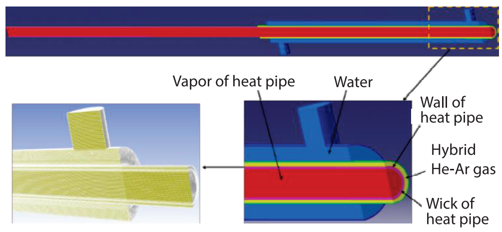

Figure 12. The CFD simulation of lithium heat pipe experimental facility

Boundary conditions

The *k*-*ε* RNG turbulence model is adopted to perform the numerical simulations. A heat flow boundary condition is assumed at the outer surface of the evaporation section, as well as the mass inlet of cooling water and the water outlet pressure. Due to the high temperature of the outer wall of the lithium heat pipe, the radiation of the condensation section of the heat pipe cannot be ignored. Considering the molecular structure symmetry of argon and helium, they cannot emit and absorb radiation energy, S2S radiation mode is selected herein. Grid sensitivity analysis has been done to obtain the fine mesh.

Results and discussions

Design power steady operation test of the lithium heat pipe

Figure 13 shows the vapor temperature variations of lithium heat pipe *vs.* different cooling water flow rates, and the heating power is 10 kW, the hybrid helium-argon gas was in different helium volume ratios. For each helium volume ratio, the vapor temperature of lithium heat pipe decreases with increasing cooling water flow rate, and the lower the cooling water flow rate is, the greater effect of flow on the vapor temperature of lithium heat pipe can be. When the cooling water flows rate increases to a certain extent, the vapor temperature of the lithium heat pipe tends to be stable. The reason is that at a low flow rate, the thermal resistance of convection heat transfer of cooling water is large and it accounts for a large proportion of the total thermal resistance of lithium heat pipe. The change of thermal resistance of convection heat transfer has a great impact on the whole heat pipe. With the increase of the flow rate, the convective thermal resistance of the cooling water decreases, and the proportion of the convective thermal resistance to the total thermal resistance decreases, so that reducing the convective thermal resistance by increasing the flow rate of the cooling water has little effect on the total thermal resistance. Therefore, when the temperature of the lithium heat pipe decreases to a certain level, increasing the cooling water flow cannot reduce the working temperature of the lithium heat pipe obviously. For each cooling water flow rate, the vapor temperature of the lithium heat pipe decreases with the increasing helium volume rate in the mixed gas. This is because the thermal conductivity of helium is higher than that of argon. Therefore, changing the volume proportion of helium is effective to adjust the working temperature of lithium heat pipe. Since the heat pipe works around 1700 K, it is suggested that the proportion of helium volume in the mixture can be around 80%, as shown in fig. 13. Figure 14 shows the change of outlet temperature of cooling water under different cooling water flow rates when the heat pipe is heated by power of 10 kW and the mixed gas is in different helium volume ratios.

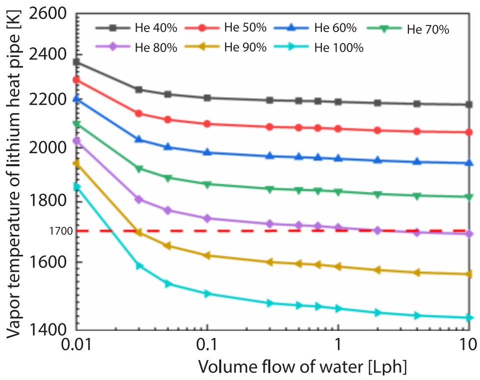

Figure 13. Variation in vapor temperature of lithium heat pipe

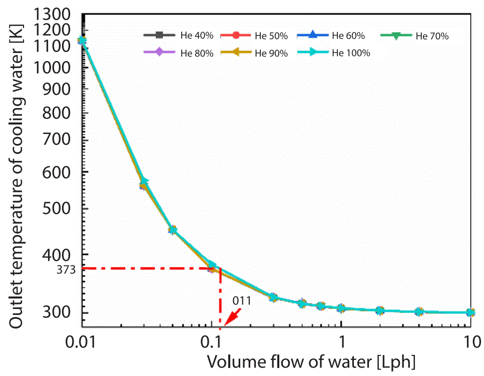

Figure 14. Variation in outlet temperature of cooling water

Increasing cooling water flow, the outlet temperature of cooling water decreases, and the outlet temperature eventually tends to be approaching the inlet value. To prevent water boiling, the outlet temperature should be lower than 373 K as much as possible. Therefore, it is suggested that the cooling water flow should be greater than 0.11 Lph. For each cooling water flow rate, the volume proportion of helium almost does not affect the outlet temperature of cooling water. This is mainly due to the constant heating power on the heat pipe.

Figure 15 shows the temperature distribution of the lithium heat pipe experimental facility when the heating power is 10 kW, the volume proportion of helium is 80%, and the cooling water flow is 0.7 Lph. It can be seen that the lowest temperature of the whole system is about 300 K in the cooling water area, and the highest temperature is about 1700 K in the lithium heat pipe. The internal temperature uniformity of the cooling water and lithium heat pipe are good, and the main temperature difference occurs in the hybrid helium-argon gas area. This is because the thermal resistance of the whole heat pipe cooling system is mainly determined by the thermal resistance of the mixed gas.

Figure 16 shows the temperature distribution of the lithium heat pipe. The temperature difference of the whole heat pipe is about 20 K, which indicates that the heat pipe has good temperature uniformity and it can be seen from fig. 16. The temperature difference in the vapor area is very small, and the main temperature difference exists in the evaporation section and condensation section. This further indicates that the thermal resistance of the heat pipe is mainly radial thermal resistance.

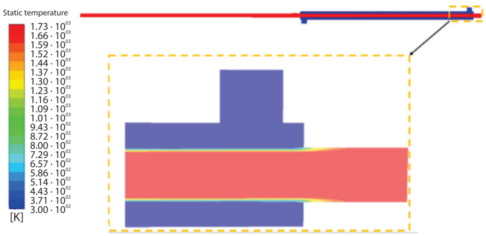

Figure 15. Temperature distribution of the experimental facility

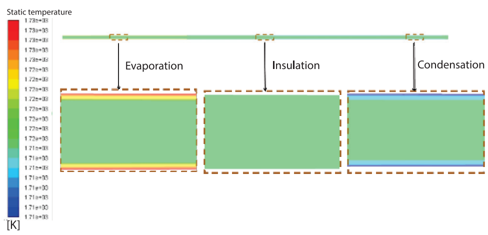

Figure 16. Temperature distribution of the lithium heat pipe

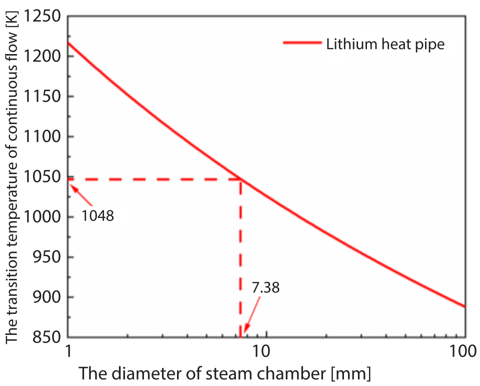

Figure 17. Transition temperatures *vs.* diameter of vapor chamber

Power shifting transients of the lithium heat pipe

Vapor flow in lithium heat pipe is considered as a continuous flow during steady-state and power shifting transients, because it is a precondition for eqs. (9) and (10). Figure 17 shows the relationship of continuous-flow transition temperatures of the lithium heat pipe *vs.* different vapor chamber diameters. The diameter of the vapor chamber of the lithium heat pipe in this design is 7.38 mm. Theorefore, the lithium heat pipe should keep temperature higher than 1048 K in the power shifting transients.

Another precondition for lithium heat pipe in power shifting transients is that the heating power must be lower than the minimum heat transfer limit among all. Figure 18 shows the variation of the heat transfer limit power for different working temperatures. When the heating power of the lithium heat pipe is 5 kW, the lowest heat transfer limit may be viscosity limit and sonic limit. Therefore, to meet previous two requirements, the working temperature of the lithium heat pipe should be higher than 1374 K in power shifting transient. In the test, helium volume ratio is 80%, the cooling water flow is 0.7 Lph, and the heating power shifts from 10-5 kW. Transient solver in CFD is used to study the working characteristics of the lithium heat pipe during an unsteady-state.

Figure 19 shows the change of the vapor temperature of lithium heat pipe with time. The vapor temperature decreases with time and finally tends to be stable in around 100 seconds. The stable temperature is 1212 K. However, it can be seen from fig. 16 that when the heating power of the heat pipe is 5 kW, the working temperature of the lithium heat pipe must be higher than 1374 K. Therefore, when the lithium heat pipe works during power shifting transient, the cooling conditions should be adjusted accordingly. With the increase of helium volume proportion in the mixed gas, the stable vapor temperature increases, and the time consumed in the state development changes little. The final stable vapor temperature will be higher than 1415 K for helium volume ratio less than 60%, which can be adopted in the experimental facility.

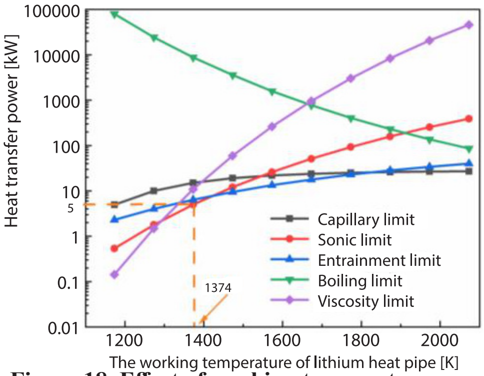

Figure 18. Effect of working temperature on heat transfer limits

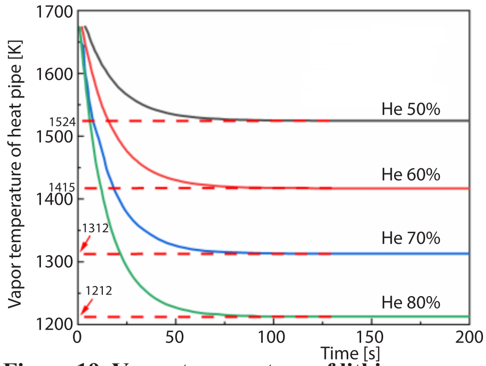

Figure 19. Vapor temperature of lithium heat pipe variations during power shifting transient

Conclusions

To serve the development of heat pipe space nuclear reactor at Institute of Nuclear Energy Safety Technology, a lithium heat pipe based experimental facility was designed and numerically verified in this paper. The simplified mathematical model of lithium heat pipe was proposed and the 3-D CFD approach was used to simulate the lithium heat pipe based experimental facility. Main results are concluded as follows.

- The numerical predictions agree well with the existing models and experimental results, the differences between them are 2% range and 5% range, respectively, which verified the correctness of the heat pipe model.
- The thermal resistance of the experimental system and the working temperature of the heat pipe can be reduced by increasing the helium volume ratio. If the working temperature is too high, the heat pipe could possibly burn out. However, it cannot start-up at too low temperatures. Therefore, helium volume ratio about 70-90% is suitable for the lithium heat pipe.
- The working temperature range of the heat pipe can be controlled by changing the flow rate of cooling water. It is viable to reduce the working temperature by increasing the flow rate of cooling water. However concerning to boiling of the cooling water, the flow rate should be higher than 0.11 Lph.
- When the heating power of the lithium heat pipe shifts from 10-5 kW, the cooling conditions should be adjusted to prevent the heat pipe from exceeding the heat transfer limits, as well as keep operating below the continuous-flow transition temperature, on the sake of long-term working safety of the heat pipe. Helium volume ratio within the range of 50-60% best applies in the current design.

Acknowledgment

This work was supported by the CASHIPS Director's Fund (Grant No. YZJJ2021QN36).

Nomenclature

C – effective volumetric heat capacity of wick
k – effective thermal conductivity of wick
r – radial co-ordinate
T – temperature
z – axial co-ordinate

Greek symbols

ε – porosity of wick
φ – circumferential co-ordinate

Subscripts

l – liquid
s – wick,
v – vapor
w – wall

References

[1] Yuan, J., *et al*., Study on Startup Characteristics of Heat Pipe Cooled and AMTEC Conversion Space Reactor System, *Progress in Nuclear Energy*, *86* (2016), Jan., pp. 18-30
[2] Sun, H., *et al*., Conceptual Design and Analysis of a Multipurpose Micro Nuclear Reactor Power Source, *Annals of Nuclear Energy*, *121* (2018), Nov., pp. 118-127
[3] Mcclure, P., *et al*., Mobile Heat Pipe Cooled Fast Reactor System Los Alamos Nat. Lab., Los Alamos, N. Mex., USA, 2014
[4] Faghri, A., *Heat Pipe Science and Technology*, CRC Press, Washington, D.C., USA, 1995
[5] Liu, X., *et al.*, Core Thermal-Hydraulic Evaluation of a Heat Pipe Cooled Nuclear Reactor, *Annals of Nuclear Energy*, *142* (2020), 107412
[6] PMcclure, P. R., *et al*., Design of Megawatt Power Level Heat Pipe Reactors, LA-UR-15-28840, Los Alamos, N. Mex., USA, 2015
[7] Gibson, M. A., *et al*., Kilopower Reactor Using Stirling Technolog Y (KRUSTY) Nuclear Ground Test Results and Lessons Learned, NASA/TM-2018-219941, 2018
[8] Gibson, M. A., *et al*., The NASA's Kilopower Reactor Development and the Path to Higher Power Missions, Aerospace Conference, NASA, Washington, USA, 2017
[9] Levinsky, A., *et al*., Westinghouse eVinciTM Reactor for off-Grid Markets, American Nuclear Society Winter Meeting 2018, Orlando, Fla., USA, 2018
[10] Hernandez, R., *et al*., Micro Heat Pipe Nuclear Reactor Concepts: Analysis of Fuel Cycle Performance and Environmental Impacts, *Annals of Nuclear Energy*, *126* (2019), Apr., pp. 419-426
[11] Sukchana, T., Jaiboonma, C., Effect of Filling Ratios and Adiabatic Length on Thermal Efficiency of Long Heat Pipe Filled with R-134a, *Energy Procedia*, *34* (2013), 1, pp. 298-306
[12] Mahdavi, M., *et al*, Experimental Study of the Thermal Characteristics of a Heat Pipe, *Experimental Thermal & Fluid Science International Journal of Experimental Heat Transfer Thermodynamics & Fluid Mechanics*, *93* (2018), May, pp. 292-304
[13] Khalili, M., Shafii, M. B., Experimental and Numerical Investigation of the Thermal Performance of a Novel Sintered-Wick Heat Pipe, *Applied Thermal Engineering*, *94* (2016), Feb., pp. 59-75
[14] Xiong, Y. X., *et al*., A Characteristic Study on the Start-up Performance of Molten-Salt Heat Pipes: Experimental Investigation, *Experimental Thermal and Fluid Science*, *82* (2017), Apr., pp. 433-438
[15] Lu, Q., *et al*., Preparation and Testing of Nickel-Based Superalloy/Sodium Heat Pipes, *Heat and Mass Transfer*, *53* (2017), 11, pp. 1-7
[16] Liu, C., Fabrication and Performance Evaluation of Flexible Flat Heat Pipes for the Thermal Control of Deployable Structure, *International Journal of Heat and Mass Transfer*, *144* (2019), 2, 118661
[17] Liu, Z. H., *et al*., Thermal Performance of Inclined Grooved Heat Pipes Using Nanofluids, *International Journal of Thermal Sciences*, *49* (2010), 9, pp. 1680-1687
[18] Kumaresan, G., *et al*., Experimental Study on Effect of Wick Structures on Thermal Performance Enhancement of Cylindrical Heat Pipes, *Journal of Thermal Analysis and Calorimetry*, *136* (2018), Oct., pp. 389-400
[19] Supowit, J., *et al.*, Designer Fluid Performance and Inclination Angle Effects in a Flat Grooved Heat Pipe, *Applied Thermal Engineering*, *101* (2016), May, pp. 770-777
[20] Kemme, J. E., Ultimate Heat-Pipe Performance, *IEEE Trans. Electron. Devices*, *16* (1969), 8, pp. 717-723

[21] Li, C., *et al*., Evaporation/Boiling in Thin Capillary Wicks (l) – Wick Thickness Effects, *Journal of Heat Transfer*, *128* (2006), 8, 1312
[22] Li, C., Peterson, G. P., Evaporation/Boiling in Thin Capillary Wicks (II) – Effects of Volumetric Porosity and Mesh Size, *Journal of Heat Transfer*, *128* (2006), 12, pp. 1320-1328
[23] Seo, J.,, Lee, J.-Y., Length Effect on Entrainment Limitation of Vertical Wickless Heat Pipe, *International Journal of Heat and Mass Transfer*, *101* (2016), Oct., pp. 373-378
[24] Wang, C. L., *et al*., Experimental Study on Startup Performance of High Temperature Potassium Heat Pipe at Different Inclination Angles and Input Powers for Nuclear Reactor Application, *Annals of Nuclear Energy*, *136* (2020), Feb., 107051
[25] Miao, S., *et al*., Experimental Study on Thermal Performance of a Bent Copper-Water Heat Pipe, *International Journal of Aerospace Engineering*, *2020* (2020), ID8632152
[26] Baraya, K., *et al*., Heat Pipe Dryout and Temperature Hysteresis in Response to Transient Heat Pulses Exceeding the Capillary Limit, *International Journal of Heat and Mass Transfer*, *148* (2020), Feb, 119135
[27] Wang, C., *et al*., Experimental Study on Heat Transfer Limit of High Temperature Potassium Heat Pipe for Advanced Reactors, *Annals of Nuclear Energy*, *151* (2021), Feb., 107935
[28] Bernades, M. A. dos S., *Developments in Heat Transfer*, InTech, Rijeka, Croatia, 2011
[29] Reay, D. A., *et al*., *Heat Pipes Theory Design & Applications*, Butterworth-Heinemann, Burlington, Canada, 2006
[30] Tournier, J. M., El-Genk, M. S., Startup of a Horizontal Lthium-Molybdenum Heat Pipe from a Frozen State, *International Journal of Heat & Mass Transfer*, *46* (2003), 4, pp. 671-685
[31] Merrigan, E. S. *et al*.,Transient Performance Investigation of a Space Power System Heat Pipe, *Proceedings*, 4th Thermophysics and Heat Transfer Conference, Boston, Mass., USA, 1986
[32] Chi, S. W., *Heat Pipe Theory and Practice*, Hemisphere Pub., New York, USA, 1976
[33] Dunn, P. D., Reay, D. A., *Heat Pipes*, Pergamon Press, New York, USA, 1978
[34] ***, S.P.o. China, Niobium and Niobium Alloy Seamless Tubes, in, Standards Press of China, Beijing, China, 2007
[35] ***, S.P.o. China, Testing Method for Heat Transfer Performance of Heat Pipes, in, Standards Press of China, Beijing, Chna, 2008
[36] Wang, C. L., *et al.*, Study on the Characteristics of the Sodium Heat Pipe in Passive Residual Heat Removal System of Molten Salt Reactor, *Nuclear Engineering and Design*, *265* (2013), Dec., pp. 691-700
[37] Cao, Y., Faghri, A., A Numerical Analysis of High-Temperature Heat Pipe Startup From the Frozen State, *Journal of Heat Transfer*, *115* (1993), 1, pp. 247-254
[38] Zuo, Z. J., Faghri, A, A Network Thermodynamic Analysis of the Heat Pipe, *International Journal of Heat and Mass Transfer*, *41* (1998), 11, pp. 1473-1484
[39] Faghri, A., Harley, C, Transient Lumped Heat Pipe Analyses, *Heat Recovery Systems and CHP*, *14* (1994), 4, pp. 351-363
[40] Cao, Y., Faghri, A., Transient 2-D Compressible Analysis for High-Temperature Heat Pipes with Pulsed Heat Input, *Numerical Heat Transfer Part A Applications*, *18* (1991), 4, pp. 483-502

Paper submitted: May 28, 2021
Paper revised: July 13, 2021
Paper accepted: July 16, 2021